Geomechanics and Engineering, *Vol. 36, No. 6 (2024) 575-587*
https://doi.org/10.12989/gae.2024.36.6.575

The contact loads inversion between surrounding rock and primary support based on dynamic deformation curve of a deep-buried tunnel with flexible primary support in consideration

Jian Zhou[1,2], Yunliang Cui*[1,2], Xinan Yang[3a], Mingjie Ma[3b] and Luheng Li[3c]

[1]*Department of Civil Engineering, Hangzhou City University, Hangzhou 310015, China*
[2]*Key Laboratory of Safe Construction and Intelligent Maintenance for Urban Shield Tunnels of Zhejiang Province, Hangzhou City University, Hangzhou 310015, China*
[3]*The Key Laboratory of Road and Traffic Engineering, Ministry of Education, Tongji University, Shanghai 201804, China*

(*Received October 8, 2024, Revised February 8, 2024, Accepted February 28, 2024*)

Abstract. The contact pressure between the surrounding rock and the support is an important indicator of the surrounding rock pressure. There has been a bottleneck in the prediction of contact loads between surrounding rock and primary support in deep-buried mountain tunnels. The main reason is that a reliable method wasn't existed to quantify the contact loads. This study had been taken into account the flexible support role of the primary support, and the fitting curve of surrounding rock deformation for dynamic tunnel construction was proposed. New formulas for the calculation of contact loads between surrounding rock and primary support were obtained by inversion. Comparative analysis of the calculation results with numerical simulation verified the reliability of the calculation method in this study. It can be seen from the analyses that the contact load between surrounding rock and primary support increases, remains unchanged and decreases during acceleration, uniform velocity and deceleration, respectively, and the deformation of the surrounding rock in the acceleration and deceleration stages cannot completely converted into contact loads. The contact loads between surrounding rock and primary support of medium-strength and weak surrounding rock tunnels are generally within 150 kPa and 1 MPa, respectively. For tunnels with weak surrounding rock, advanced support can be installed to reduce the unique release coefficient λ_0 and the value of the constant D, with the purpose of reducing the contact loads between surrounding rock and primary support. Changes in support parameters have a small effect on the contact loads between surrounding rock and primary support, but increase or decrease the safety factor, resulting in a waste of resources or a situation that threatens the safety of the support. The results of this research provide guidance for the prediction of contact loads between surrounding rock and primary support for dynamic tunnel construction.

Keywords: contact load; fitted curve; flexible support; inversion; mountain tunnel

1. Introduction

The NATM is a tunnelling method proposed in the 1950s by the Austrian scholar Rabcewicz (1964), who emphasized the use of flexible support to evaluate the bearing capacity of the surrounding rock itself. Currently, the bearing capacity of the support structure is generally evaluated by measuring the contact pressure between the surrounding rock and the support structure. The contact pressure reflects the reasonableness of the force of the supporting structure which has a greater impact on the safety of tunnel construction support. However, contact pressure is based on field monitoring which lacks a reliable theoretical method for quantifying the contact loads between surrounding rock and primary support. Primary support loads are generally obtained by field monitoring of the contact loads between surrounding rock and primary support, but load monitoring is not a mandatory part of the project. The contact loads between the surrounding rock and the primary support are generally not known during the construction process. Of course, there are empirical formulas for predicting support loads in the relevant codes, but it is not clearly reasonable to base support loads on the relevant dimensional and rock parameters of the tunnel alone. In addition, much literature has been conducted to explore the theories of tunnel construction (Fahimifar *et al.* 2015, Ranjbarnia *et al.* 2020, Chinaei *et al.* 2021, Zhou *et al.* 2021a, Moon *et al.* 2022, Zhou *et al.* 2023a, b, Hu *et al.* 2023, Zhang *et al.* 2024). However, few literature deals with support load calculations. Little literature has shown that the installation time of the support structure also has a significant effect on the support structure loads (Miranda *et al.* 2015, Liu *et al.* 2018, Dehnavi and Sadeghi 2019), but a quantitative relational equation has not been given. Thus, there is an urgent need to propose a novel method for quantifying the contact loads between surrounding rock and primary support.

For a long time, in order to quantify the support loads,

*Corresponding author, Professor
E-mail: cuiyl@hzcu.edu.cn
[a]Professor
[b]Ph.D.
[c]Ph.D.

ISSN: 2005-307X (Print), 2092-6219 (Online)

many scholars have conducted researches related to support loads by drawing on the elastoplastic theories of the roadway. For example, Carranza-Torres and Fahimifar (1999), Park and Kim (2006), Serrano *et al.* (2011), Feng *et al.* (2014), Zhang *et al.* (2019) derived analytical expressions for stress and displacement in the plastic zone of the surrounding rock of a circular chamber. However, the support pressures were not the focus of the above researches, which was given as a known parameter. Many scholars brought in the interaction between the surrounding rock and the support structure under the dynamic construction effect of tunnels. Based on the convergence-confinement method, the support load can be solved as an unknown value, which further improves the elastoplastic analytical theories of deep-buried tunnels. Cai *et al.* (2015) obtained an analytical solution of tunnel excavation stresses and displacements by considering the contact surface coupling between the anchors and the surrounding rock.

The results indicate that the location of the neutral point of the anchor is related to the length of the anchor and the radius of the tunnel, which is significantly affected by the mechanical properties of the rock mass itself. Oreste (2003a) proposed a stress and displacement solution for the strength and stiffness of shotcrete under the action of shotcrete-bolt composite lining with gradual hardening over time. Shen *et al.* (2019) proposed an improved method for calculating lining pressure and deformation by dividing the convergence-confinement method into two stages. It can be seen that the final pressure reduction on the lining can be done by reducing the lining stiffness and delaying the installation time. The above researches generally multiply the stiffness of the support structure by the deformation generated after the support structure is installed to obtain the support load, which is not applicable to the flexible shotcrete-bolt support. For example, as a kind of flexible support structure, shotcrete has the characteristic of "resisting and yielding at the same time". So, the convergence-confinement method is not applicable, and the gap between its calculation results and measured data is too large or even reaches two orders of magnitude. Thus, the current contact loads calculation between surrounding rock and primary support has not yet considered the flexible characteristics of shotcrete.

In view of the above analysis, it is necessary to start from the formation mechanism of the contact loads between surrounding rock and primary support. The contact load is closely related to the dynamic deformation of the surrounding rock-support interaction. Zhang and Chen (2016) elaborated the characteristics of the surrounding rock in detail from the perspective of kinematics of the surrounding rock, which pushed forward the development of the primary support load mechanism. However, the quantitative relationship between the contact load and the deformation of the surrounding rock was not given, and there is still much room for the development of the contact loads prediction between surrounding rock and primary support. Therefore, the flexible characteristics of the primary support can be understood from the perspective of kinematics of the surrounding rock-primary support so as to calculate the contact loads between surrounding rock and primary support more accurately.

From the longitudinal deformation curves (LDP) of the tunnel construction, it is known that the deformation of the surrounding rock is not only generated after the tunnel excavation, but also within a section in front of the excavation face. The loads on the primary support is an indirect response to the pre-deformation of the surrounding rock (Vlachopoulos and Diederichs 2009, Prassetyo and Gutierrez 2018, Zhang *et al.* 2019, Shen *et al.* 2019, Fan *et al.* 2021). The deformation of the surrounding rock is firstly in the accelerated stage due to pre-deformation, and then it presents the state of uniform deformation-decelerated deformation. It is clarified the relationship between the deformation of the surrounding rock in different motion states and the loads at the contact surface between surrounding rock and primary support. A reliable calculation method of the contact loads between surrounding rock and primary support will be obtained.

Therefore, this research project is planned to invert the contact loads between surrounding rock and primary support based on the dynamic deformation curve of the surrounding rock with the flexible support characteristics of the primary support in consideration. A quantitative formula for the calculation of contact loads between surrounding rock and primary support can be proposed. It verifies by numerical simulation method subsequently. The results of the study can provide guidance for predicting the contact loads on the between surrounding rock and primary support of deep-buried medium-strength or soft surrounding rock tunnels.

2. Characteristics of the deformation curve of the surrounding rock for dynamic tunnel construction

To obtain the calculation formula of contact loads between surrounding rock and primary support, it is necessary to clarify the relationship between the deformation of tunnel surrounding rock and contact load. Firstly, the change law of surrounding rock deformation during tunnel construction can be explored. According to the convergence-confinement method, the deformation of the tunnel along the excavation direction is not homogeneous. Due to the existence of the excavation surface, the surrounding rock displacement within 1.5 times of the tunnel diameter plays a certain constraining role, which is generally referred to as the spatial effect (Carranza-Torres 2000). As a result, the deformation of the surrounding rock in the vicinity of the excavation face is much smaller compared to the final deformation of the surrounding rock. The longitudinal deformation curve of the tunnel can be plotted as shown in Fig. 1. From Fig. 1, it is obvious to find that the deformation of the surrounding rock in front of the excavation face has already appeared, which is generally called pre-deformation. The deformation of the surrounding rock at the back of the excavation surface presents the process of sharp increase-growth tends to slow down-deformation stabilization. The deformation at the excavation surface and the final deformation of the surrounding rock are denoted as u_0 and u_∞ respectively, and the distance from the excavation surface is denoted as X.

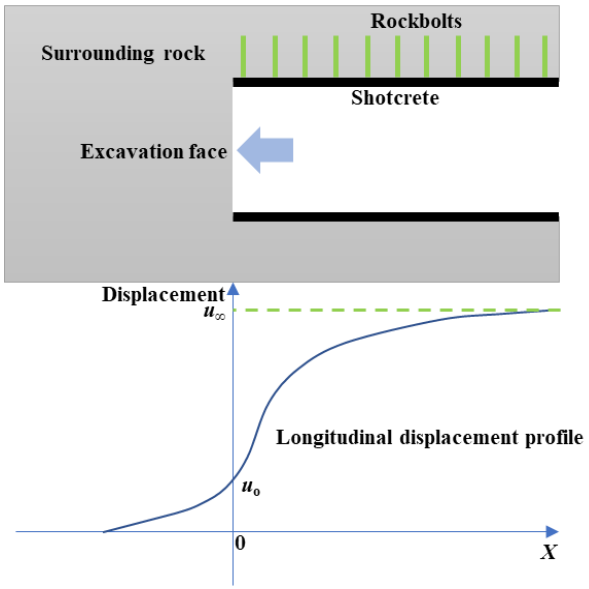

Fig. 1 Longitudinal deformation curve of the tunnel

In order to describe the relationship between the surrounding rock displacement at a point in the longitudinal direction of the tunnel and the final displacement of the surrounding rock, the displacement release coefficient λ is defined as the value of the surrounding rock deformation of the tunnel wall at a certain distance X from the excavation surface at a certain point and the ratio to the final deformation of the surrounding rock. It can be expressed by the following formula.

$$\lambda(X)=u(X)/u(\infty) \tag{1}$$

where $u(X)$ is the value of surrounding rock deformation at monitoring point X. $u(\infty)$ represents the stable deformation of surrounding rock at monitoring point X.

For the displacement release coefficient, some scholars have also carried out research. Panet (1995) obtained the displacement release coefficient in the unsupported state based on the theory of elastic deformation of the surrounding rock after excavation. Displacement release coefficient can be given by

$$\lambda=0.25+0.75\left[1-\left(\frac{0.75}{0.75+X/r_0}\right)^2\right] \tag{2}$$

where r_0 is the radius of a tunnel.

The empirical equation for the displacement release coefficient given by Hoek (2001) using the best-fit method with field measured data from the Mingtam underground hydropower station can be written as

$$\lambda=\left[1+\exp\left(\frac{-X/r_0}{1.10}\right)\right]^{-1.7} \tag{3}$$

Eqs. (2) and (3) can only better reflect a certain part of the deformation, such as the deformation of the surrounding rock in front of or behind the excavation, which cannot reflect the deformation of the whole process during the tunnel excavation. Vlachopoulos and Diederichs (2009) proposed an expression for the displacement release coefficients of ideal elastoplastic surrounding rock, and Alejano *et al.* (2012) further verified that the formula is also applicable in the strain-softening surrounding rock is also applicable. The formula is more reasonable and widely used because it discusses the displacement release coefficient before and after excavation separately. The expression can be given by

$$\lambda(X)=\begin{cases}1-(1-\lambda_0)\exp\left[-3X/\left(2r_0R^*\right)\right] & X\geq 0\\ \lambda_0\exp\left(X/r_0\right) & X<0\end{cases} \tag{4}$$

where λ_0 represents displacement release coefficient at the excavation face and $\lambda_0=\frac{1}{3}\exp\left(-0.15R^*\right)$. $R^*=R_{\text{pmax}}/r_0$ and R_p is the radius of the maximum plastic zone of the surrounding rock in the absence of support.

The displacement release coefficients for the above studies are generally given based on unsupported conditions. Since the support structure is installed during the tunnel excavation, then there is a change in the formula for the displacement release coefficient behind the excavation face. Eq.(4) can be further adjusted as

$$\lambda(X)=\begin{cases}1-(1-\lambda_0)C\exp(-AX/r_0) & X\geq 0\\ \lambda_0\exp\left(DX/r_0\right) & X<0\end{cases} \tag{5}$$

where A, C and D represent constants which are all greater than 0.

In addition, it is appropriate to fit the longitudinal deformation curve of the surrounding rock based on Eq.(5) for the primary support immediately following the excavation face. However, for moderate condition and better surrounding rocks, the primary support installation generally lags behind the excavation face by a certain distance. In the excavation face to the point where the primary support is installed to the surrounding rock stress release without any support restriction, the surrounding rock is still doing accelerated movement in this range, and the displacement fitting curve is consistent with the pre-deformation stage. At this point, the unique release coefficient $\lambda(X)$ can be further adjusted as follows.

$$\lambda(X)=\begin{cases}1-(1-\lambda_0)C\exp(-AX/r_0) & X\geq X^*\\ \lambda_0\exp\left(DX/r_0\right) & X<X^*\end{cases} \tag{6}$$

where X^* is defined as the distance from the excavation surface at which the support is installed.

Combining Eq. (1), the surrounding rock deformation $u(X)$ can be obtained.

3. Calculation method of contact loads between surrounding rock and primary support

3.1 Calculation method of contact loads between surrounding rock and primary support when the surrounding rock is in accelerated motion

The next step is to obtain the contact loads between surrounding rock and primary support. The contact load is generally obtained by multiplying the deformation of the surrounding rock after the primary support is installed with the stiffness of the primary support, with the following equation.

$$p_{\mathrm{ini}}(X) = K_{\mathrm{ini}} \Delta u(X) \tag{7}$$

where $p_{\mathrm{m}}(X)$ denotes the contact loads between surrounding rock and primary support. $\Delta u(X)$ represents the deformation of the surrounding rock produced after the installation of the primary support. K_{ini} is the stiffness of the primary support. For composite lining, the rockbolts form a composite carrier with the surrounding rock. Thus, the shotcrete loads should not include the effect of the rockbolts. Moreover, in medium-strength and better surrounding rock conditions where steel arches are generally not used, only the shotcrete stiffness is in consideration, with the following expression (Oreste 2003b).

$$K_1 = \frac{E_1\left(r_0^2 - r_1^2\right)}{\left(1+\mu_1\right)\left[\left(1-2\mu_1\right)r_0^2 + r_1^2\right]}\frac{1}{r_0} \tag{8}$$

where E_1 and r_1 are the elastic modulus and internal diameter of shotcrete, respectively. μ_1 is the Poisson's ratio of shotcrete.

For weak surrounding rock, the role of steel arch needs to be considered in addition to shotcrete, and the stiffness of steel arch has the following formula (Zhou and Yang 2021b).

$$K_{12} = \frac{E_{\mathrm{st}} A_{\mathrm{set}}}{S\left(r_0 - h_{\mathrm{set}}/2\right)^2} \tag{9}$$

where E_{st}, A_{set}, S and h_{set} are the elastic modulus, cross-sectional area, layout spacing and section height of the steel arch, respectively.

However, there is a problem in Eq.(6), that is, the primary support is regarded as rigid support and the flexible support of shotcrete is ignored. This situation completely transforms the radial displacement generated by the surrounding rock into the load generated by the shotcrete itself, and the calculation results are far from the actual situation. In fact, the surrounding rock load is released in the process of "resisting and yielding at the same time" of the primary support, and the contact loads between surrounding rock and primary support also increase with the increase of surrounding rock deformation. Therefore, there is no necessary relationship between the contact loads on primary support and surrounding rock deformation.

Similar to Newton's second law, when pushing an object, the force required for uniform linear motion is set to F1. Then, if an object is in acceleration motion, the push force exerted on the object must be greater than F1. Similarly, when the object is in deceleration motion, the push force exerted on the object must be less than F1. Therefore, the acceleration of the movement of the surrounding rock can be obtained from the deformation curve equation of the surrounding rock to judge the increase or decrease of the contacts load between the surrounding rock and primary support. The second-order derivation of Eq. (6) yields the acceleration of the deformation of the surrounding rock as

$$u''(X) = \begin{cases} -(1-\lambda_0)\dfrac{A^2}{r_0^2}\exp(-AX/r_0)u(\infty) & X \geq X^* \\ \dfrac{\lambda_0}{r_0^2}\exp(X/r_0)u(\infty) & X < X^* \end{cases} \tag{10}$$

It is clearly to see that when $X < X^*$, $u''(X) > 0$. The accelerated movement of the surrounding rock in front of the excavation face indicates that the virtual support load on the profile of the tunnel section is gradually increasing. when $X \geq X^*$, $u''(X) < 0$. Then, the surrounding rock moves at a decelerating speed behind the excavation face. However, it is not difficult to find that the surrounding rock basically shows a uniform velocity movement for a period of time after the primary support is installed, and only after that will it show a significant deceleration movement. Thus, according to the actual deformation curve of the surrounding rock, the contact loads between surrounding rock and primary support should present the process of increasing-unchanging-decreasing.

However, a large amount of monitoring data indicates that when the pressure box is placed between the shotcrete and the surrounding rock, the contact loads between the surrounding rock and the primary support shows that it starts to increase from 0 and tends to stabilize eventually. In fact, due to the hysteresis of load transfer, the pressure value presented by the pressure box gradually increases from 0 to the load when the primary support is just installed. It needs a process which is not achieved overnight. Although the shotcrete loads monitored on site

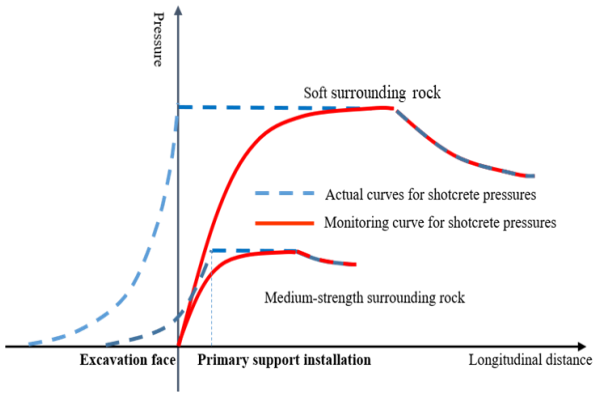

Fig. 2 Comparison of the actual path of the contact loads between the surrounding rock and the primary support with the field measurements

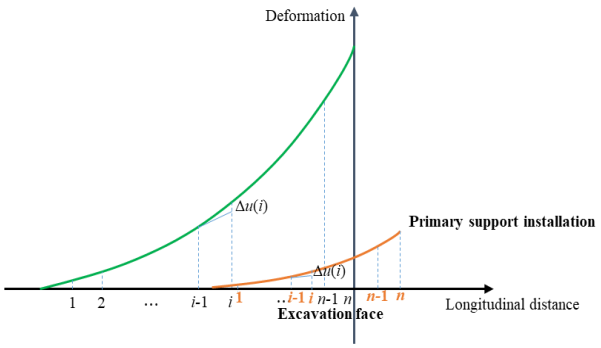

Fig. 3 Schematic diagram of calculation of contact loads between the surrounding rock and the primary support

differed from the actual path of development, the final results tended to be consistent. Thus, the effect of the comparison between the actual path of the contact loads between the surrounding rock and the primary support and the field measurement can be shown in Fig. 2. This research can provide a new idea for the prediction of the contact loads between the surrounding rock and the primary support in tunnels.

In the case of weak or moderate strength surrounding rock, the surrounding rock is accelerated during the pre-deformation phase or before the primary support is installed. If there is a virtual primary support structure at this time, its load is accelerated, but not all deformation is converted into load at this stage. If the surrounding rock moves at a uniform speed, the contact loads between the surrounding rock and the primary support remains unchanged, which reflects the flexible support of the primary support structure. Only the deformation generated when the surrounding rock moves at an accelerated speed minus the deformation generated at a uniform speed is considered to be the increased load on the contact surface of the surrounding rock and the primary support. Therefore, the calculation of the contact loads between the surrounding rock and the primary support when the surrounding rock carries out accelerated movement can be based on the calculation shown in Fig. 3.

From the Fig. 3, the surrounding rock deformation is divided into n segments in the stage of accelerated movement. The general range of pre-deformation is generally in front of the excavation face r_0 , so the length of each segment of the soft surrounding rock or medium-strength surrounding rock is $3r_0/n$. For section i the displacement increment associated with the contact loads between the surrounding rock and the primary support is $\Delta u(i)$, which can be obtained by subtracting the actual displacement at the end of section i from the actual deformation at the end of section i-1 due to the uniform velocity movement of the surrounding rock. The deformation of the surrounding rock during the accelerated motion stage has the following equation.

$$u(X)=\lambda_0\exp(DX/r_0)u(\infty) \tag{11}$$

Obtaining the slope of the pre-deformation of the surrounding rock by carrying out the first order derivative of $u(X)$ can be expressed as

$$\frac{\partial u(X)}{\partial X}=\frac{D\lambda_0}{r_0}\exp(DX/r_0)u(\infty) \tag{12}$$

Next, the tangent equation of i-1th segment end can be obtained, and the coordinate of the point on the displacement curve of i-1th segment end is $\left(-3r_0\frac{n+1-i}{n},u\left(-3r_0\frac{n+1-i}{n}\right)\right)$. Following this, the tangent equation of i-1th segment end can be written as

$$u_{i-1}(X)=\frac{D\lambda_0}{r_0}\exp\left(-3r_0\frac{D(n+1-i)}{n}/r_0\right)u(\infty)\left(X+3r_0\frac{n+1-i}{n}\right)+u\left(-3r_0\frac{n+1-i}{n}\right) \tag{13}$$

At this point, the value at the end of segment i can be rewritten as

$$u_{i-1}(-3r_0\frac{n-i}{n})=\frac{D\lambda_0}{r_0}\exp\left(-3r_0\frac{D(n+1-i)}{n}/r_0\right)u(\infty)\frac{3r_0}{n}+u\left(-3r_0\frac{n+1-i}{n}\right) \tag{14}$$

Then, the displacement increment $\Delta u(i)$ associated with contact load between the surrounding rock and the primary support in section i can be expressed as

$$\Delta u(i)=u\left(-3r_0\frac{n-i}{n}\right)-u_{i-1}(-3r_0\frac{n-i}{n}) \tag{15}$$

If there is no steel arch, the contact loads between the surrounding rock and the primary support in the pre-deformation stage can be written as

$$p_{\text{ini}}(X=0)=\sum_{i=1}^{n}K_1\Delta u(i) \tag{16}$$

In the presence of a steel arch, the contact loads calculation between the surrounding rock and the primary support for the pre-deformation phase can be rewritten as

$$p_{\text{ini}}(X=0)=\sum_{i=1}^{n}(K_1+K_{12})\Delta u(i) \tag{17}$$

3.2 Calculation method of contact loads between the surrounding rock and the primary support when the surrounding rock is in decelerated motion

The deformation curve of the surrounding rock generally has an obvious deceleration stage. A large number of monitoring data also respond to the contact pressure increase to a certain extent there is a tendency to decline (Liu *et al.* 2015, Sun *et al*. 2018, Tian *et al*. 2022, Guo *et al.* 2023), as shown in Fig. 4, which also provides evidence for the surrounding rock to decelerate. However, it is not the case that the surrounding rock has just entered the deceleration stage, and the contact loads calculation between the surrounding rock and the primary support also decrease. The response of the contact loads calculation between the surrounding rock and the primary support on the pressure boxes have a hysteresis compared with the

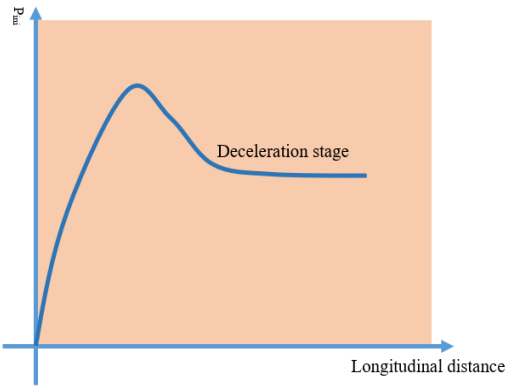

Fig. 4 Measured curves of contact loads calculation between the surrounding rock and the primary support

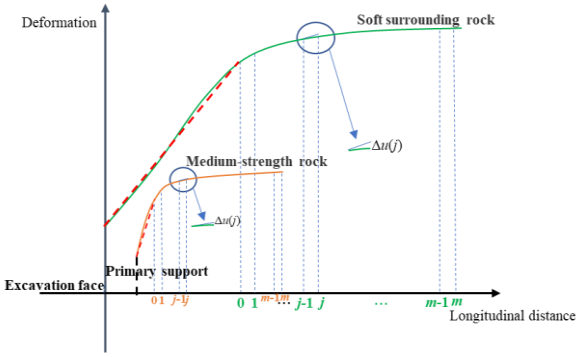

Fig. 5 Comparison of actual path of sprayed concrete load with field measurements

deformation of the surrounding rock. Since it is difficult to predict when the load enters the deceleration stage, it is planned to take the obvious deceleration section as the study point.

Similar to the calculation of contact loads calculation between the surrounding rock and the primary support during the acceleration stage of the surrounding rock, the deformation of the surrounding rock during the deceleration stage is not always converted into reduced loads when the surrounding rock decelerates significantly. The contact loads are basically unchanged when the surrounding rock is moving at a uniform speed, then the contact loads at the beginning of the apparent deceleration of the surrounding rock and at the end of the acceleration are equal. The actual deformation of the surrounding rock in relation to the reduction of the contact load is calculated when the surrounding rock is subjected to significant deceleration. The calculation of the contact load reduction can be based on the deformation curve of the surrounding rock behind the tunnel excavation surface, as shown in Fig. 5.

The deformation curves behind the excavation face in Fig. 5 discuss the medium-strength surrounding rock tunnels separately from the weak surrounding rock tunnels. Both tunnels with different surrounding rock conditions divide the decelerated deformation stage into m segments on average. The distance from the excavation surface when the surrounding rock generated obvious deceleration is X_0, and the distance from the excavation surface when the surrounding rock deformation is basically unchanged is X_1. Similar to the pre-deformation stage, each segment is of length $(X_1 - X_0)/m$. For the displacement reduction $\Delta u(j)$ associated with the contact load in section j, the displacement at j can be subtracted from the displacement at j by the tangent line at j-1 to the displacement at j of the surrounding rock deformation curve. If $X > 0$, the surrounding rock deformation has the following equation.

$$u(X) = \left[1 - (1-\lambda_0)\exp(-AX/r_0)\right]u(\infty) \tag{18}$$

Obtaining the slope of the deceleration stage of the surrounding rock by carrying out the first order derivative of $u(X)$ can be given by

$$\frac{\partial u(X)}{\partial X} = \frac{A(1-\lambda_0)}{r_0}\exp(-AX/r_0)u(\infty) \tag{19}$$

Next, the tangent equation of the surrounding rock deformation curve at j-1 is demanded. The coordinates of the surrounding rock displacement curve at j-1 is $\left(X_0 + \frac{(X_1 - X_0)(j-1)}{m}, u\left(X_0 + \frac{(X_1 - X_0)(j-1)}{m}\right)\right)$ subsequently, and then the displacement tangent equation at j-1 can be expressed as

$$u_{j-1}(X) = \frac{A(1-\lambda_0)}{r_0}\exp\left(-A\left[X_0 + \frac{(X_1 - X_0)(j-1)}{m}\right]/r_0\right)u(\infty)\left[X - \left(X_0 + \frac{(X_1 - X_0)(j-1)}{m}\right)\right] + u\left(X_0 + \frac{(X_1 - X_0)(j-1)}{m}\right) \tag{20}$$

At this time, $u_{j-1}(X)$ at j of Eq. (20) can be adjusted to

$$u_{j-1}\left(X_0 + \frac{(X_1 - X_0)j}{m}\right) = \frac{A(1-\lambda_0)}{r_0}\exp\left(-A\left[X_0 + \frac{(X_1 - X_0)(j-1)}{m}\right]/r_0\right)u(\infty)\frac{(X_1 - X_0)}{m} + u\left(X_0 + \frac{(X_1 - X_0)(j-1)}{m}\right) \tag{21}$$

Then, the displacement increment $\Delta u(j)$ associated with the contact loads between the surrounding rock and the primary support at location j can be written as

$$\Delta u(j) = u\left(X_0 + \frac{(X_1 - X_0)j}{m}\right) - u_{j-1}\left(X_0 + \frac{(X_1 - X_0)(j-1)}{m}\right) \tag{22}$$

If there is no steel arch, the final contact load between the surrounding rock and the primary support can be written as

$$p_{\text{ini}}(X = X_1) = \sum_{i=1}^{n} K_1 \Delta u(i) - \sum_{j=1}^{m} K_1 \Delta u(j) \tag{23}$$

In the presence of a steel arch, the contact load between the surrounding rock and the primary support can be rewritten as

$$p_{\text{ini}}(X = X_1) = \sum_{i=1}^{n} (K_1 + K_{12})\Delta u(i) - \sum_{j=1}^{m} (K_1 + K_{12})\Delta u(j) \tag{24}$$

4. Validation of the calculation method for contact loads between surrounding rock and primary support

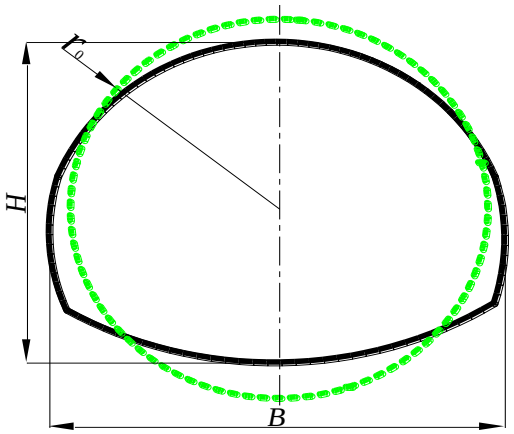

Fig. 6 Equivalent circle of a horseshoe-shaped section

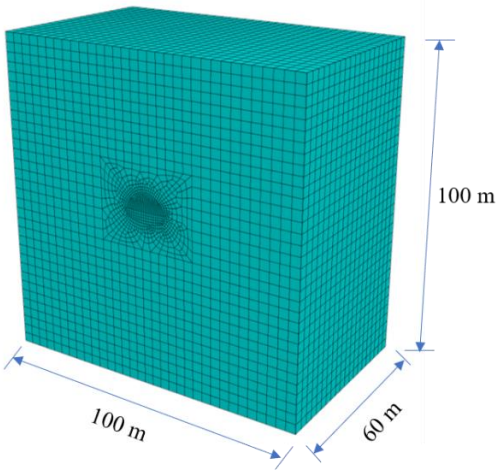

(a) 3D model

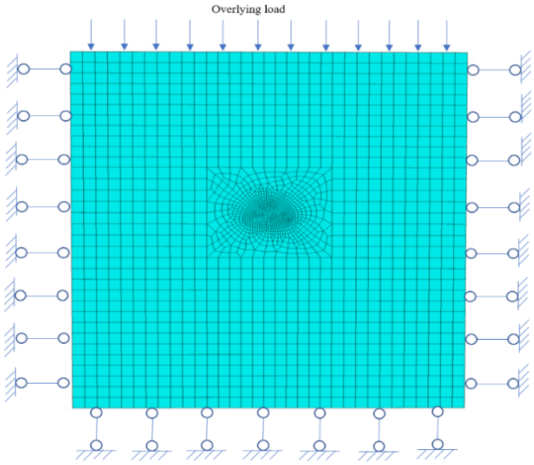

(b) Loads and constraints

Fig. 7 Tunnel modelling and boundary conditions

In order to validate the calculation method of the contact loads between surrounding rock and primary support in this research project, FLAC3D6.0 software is proposed to be used to simulate the whole process of excavation and primary support construction for two conditions of tunnels with medium-strength surrounding rock and weak surrounding rock which can be obtained the dynamic surrounding rock deformation curves of the tunnels. In the research, the calculation method is based on the inversion of the surrounding rock deformation curve for the contact loads between surrounding rock and primary support which can be compared with the numerical simulation to verify the feasibility of the calculation method. A multi-centred circular tunnel is proposed to be built with a tunnel span B of 13.35 m and a height H of 9.25 m. For the previous section dividing the acceleration and deceleration stages of the surrounding rock into n and m portions, it is proposed to take one portion for every 3 m in the longitudinal distance of the tunnel here. In addition, due to the horseshoe shaped tunnel in the numerical simulation, while the tunnel type in the theoretical analysis is circular, radius r_0 is calculated using the following equation.

$$r_0 = \frac{B+H}{4} \tag{25}$$

The radius equivalent schematic can be shown in Fig. 6. Then, the radius r_0 of the equivalent circle is 11.3 m.

The model size should reduce the boundary effect, and the boundary length should be more than three times of the tunnel diameter. Therefore, the model size is set to 100 m×60 m×100 m. The constructed model and boundary conditions can be presented in Fig. 7, and the support structure of the tunnel can be shown in Fig. 8. Moreover, the monitoring section of the tunnel is taken to be at the vault of longitudinal intermediate section.

Tunnel construction steps include the excavation of the rock mass and the installation of support, generally through the FISH language to achieve cyclic construction. For the simulation of the support structure, Shell units were created and assigned to the tunnel walls as shotcrete. If the rockbolts cannot resist the bending moment, Cable unit is used to simulate it, and Beam unit is an isotropic, linear elastic material without damage limit, which can simulate the steel arch.

The Mohr-Coulomb criterion was proposed to be used for the constitutive model of the surrounding rock. The basic design parameters of the surrounding rock were list in Table 1.

The construction parameters of the tunnel can be obtained in Table 3. The primary support of medium-strength surrounding rock was installed 6 m after the excavation face, and the primary support of soft surrounding rock was installed immediately after the excavation face by using the three-step construction method. The heights of the upper, middle and lower sections under the three-step construction conditions are 2.45 m, 3 m and 4 m, respectively.

Numerical simulation is carried out based on the longitudinal deformation curves at the vault for the above two types of surrounding rocks, and the surrounding rock displacement curves are plotted as in Figs. 9 and 10. It is clearly to find that the displacement of the surrounding rock starts from the front of the excavation and increases rapidly at the excavation surface until it stabilizes. The displacement of the medium-strength tunnel tends to

Table 1 Basic design parameters of surrounding rock

Surrounding rock grade	*Gravity of surrounding rock* /(kN/m^3)	In-Situ stress/MPa	Cohesion /MPa	Internal friction angle /°	Elastic modulus /GPa	Poisson's ratio
Medium-strength surrounding rock	24	6	10	30	15	0.3
Soft surrounding rock	18.5	6	1.5	25	5	0.25

Table 2 Basic design parameters of surrounding rock

Support structure	Parameter	Medium-strength surrounding rock	Soft surrounding rock
Shotcrete	Elastic modulus /GPa	25	25
	Poisson's ratio	0.2	0.2
	Thickness /m	0.15	0.25
Rockbolt	Elastic modulus /GPa	200	200
	Length /m	3	4
	Inter-row spacing /m	1.2	0.9
Steel arch	Elastic modulus /GPa	/	206
	Cross-sectional area /cm^2	/	39.578
	Section height /mm	/	200
	Interval /m	/	0.9

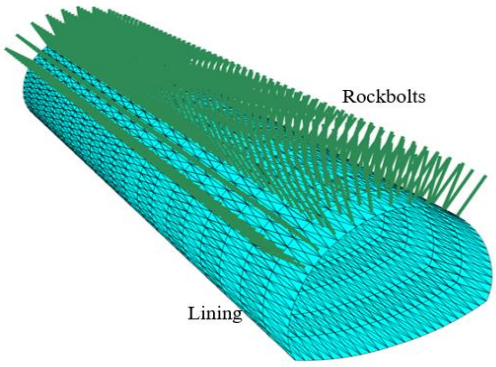

(a) Support structure for medium-strength surrounding rock

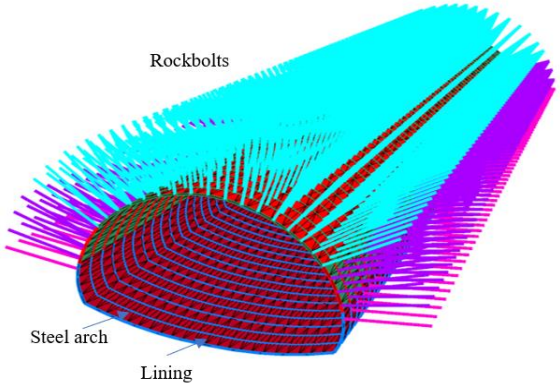

(b) Support structure for soft surrounding rock

Fig. 8 Support structure of tunnels

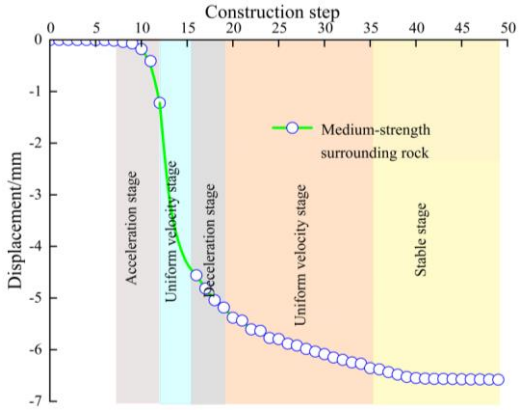

Fig.9 Deformation curve of vault in the medium-strength surrounding rock

stabilize faster, while the displacement of the weak tunnel takes a longer time to stabilize. The deformations of the tunnel with medium-strength surrounding rock and weak surrounding rock are 6.6 mm and 88.9 mm, respectively. Both of them experienced the process of accelerated motion-uniform motion-decelerated motion of surrounding rock, which is basically consistent with the kinematic analysis of surrounding rock deformation in the previous section.

Representing the apparent acceleration and deceleration stages in Figs. 9 and 10 as segmented functions, the following equations can be obtained. The function fit is above 0.98, which is a good fit.

$$\text{Medium-strength surrounding rock: } \begin{cases} u(X)=1.1385\exp(0.2905X) & \text{(Acceleration stage, } R^2=0.996) \\ u(X)=6.58-15.21\exp(-0.1264X) & \text{(Deceleration stage, } R^2=0.992) \end{cases} \tag{26}$$

$$\text{Soft surrounding rock: } \begin{cases} u(X)=11.124\exp(0.1981X) & \text{(Acceleration stage, } R^2=0.9932) \\ u(X)=89.19-1591\exp(-0.1445X) & \text{(Deceleration stage, } R^2=0.986) \end{cases} \tag{27}$$

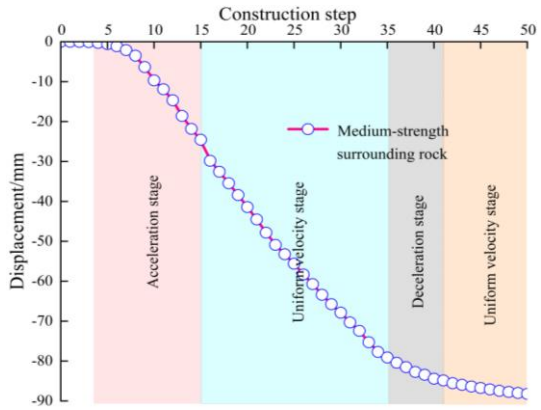

Fig. 10 Deformation curve of vault in the soft surrounding rock

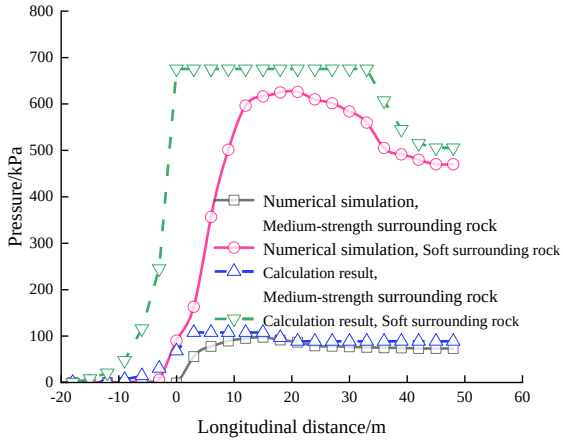

Fig. 11 Comparison between theoretical analysis and numerical simulation

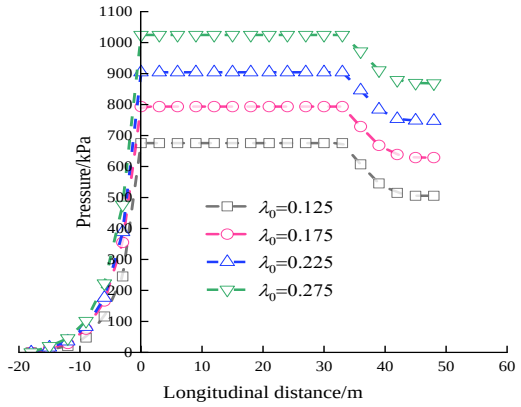

Fig. 12 Effects of λ_0 on contact loads between surrounding rock and primary support

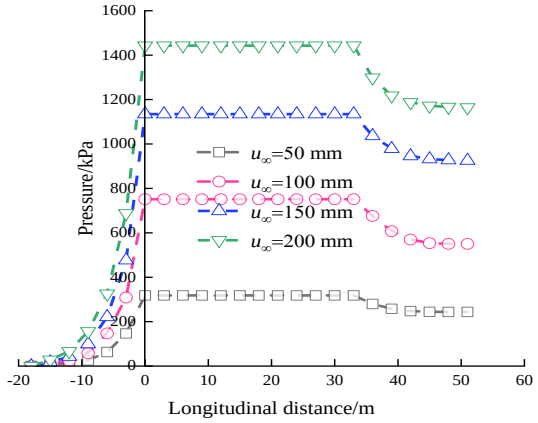

Fig. 13 Effects of $u(\infty)$ on contact loads between surrounding rock and primary support

The selection of the monitoring point for the contact loads between surrounding rock and primary support in the numerical simulation is proposed to be on the shotcrete unit at the vault of the arch at 30m in the longitudinal direction. Combined with the theoretical calculation method of the contact loads between surrounding rock and primary support in the previous section, it is analyzed in comparison with the numerical simulation results, as shown in Fig. 11.

From Fig. 11, it is obvious to see that the theoretical analyses and numerical simulations have been extremely close to each other, which presents a trend of load growth followed by a slight decrease. It is basically consistent with the description of the kinematics of the surrounding rock in this research. For the tunnel with medium-strength surrounding rock, the theoretical analysis and numerical simulation of the contact loads between surrounding rock and primary support reaches a maximum of 107.8 kPa and 97.3 kPa, respectively, with an error of about 10.7%. For the weak surrounding rock tunnels, the theoretical analysis and numerical simulation of the contact loads between surrounding rock and primary support reached 88.7 kPa and 73.1 kPa at maximum, with an error of about 7.8%. In the past, the primary support was regarded as rigid support, and the calculation results differed from the theory by 1 to 2 orders of magnitude. Therefore, the results of this research are more slightly larger than the numerical simulation results, which verifies the feasibility of the theoretical analysis. It can be used as a prediction method of the contact loads between surrounding rock and primary support.

5. Analysis of factors affecting contact loads between surrounding rock and primary support

In order to carry out the analysis of factors affecting the contact loads between surrounding rock and primary support, Eqs. (26) and (27) need to be written in the format of Eqs. (5) and (6). In this subsection, as an example of the parameters of the weak surrounding rock in the previous section, it is proposed to investigate the effects of displacement release coefficient λ_0, final displacement $u(\infty)$, and displacement constants A, C, and D on the contact loads between surrounding rock and primary support at the excavation face. Eq. (27) can be further adjusted as

$$\begin{cases} u(X)=0.125\times\exp(0.1981X)\times 89.19 \ \text{(Acceleration stage)} \\ u(X)=[1-(1-0.125)\times 20.387\times\exp(-2.239X/11.3)]\times 89.19 \ \text{(Deceleration stage)} \end{cases} \quad (28)$$

From Eq. (28), the fitting equations of λ_0, $u(\infty)$, A, C and D for the accelerated and decelerated stages of the weak surrounding rock are 0.125, 89.19 mm, 2.239, 20.387 and

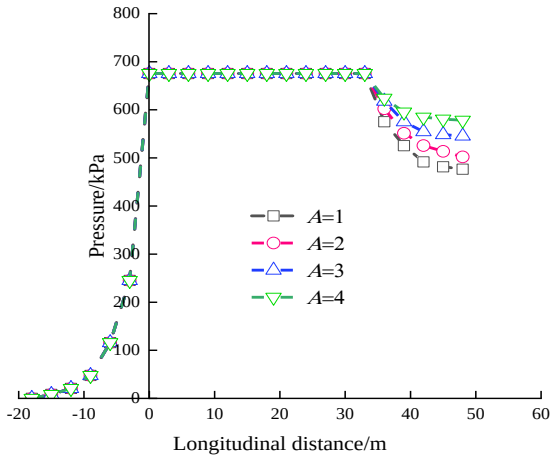

Fig. 14 Effects of A on contact loads between surrounding rock and primary support

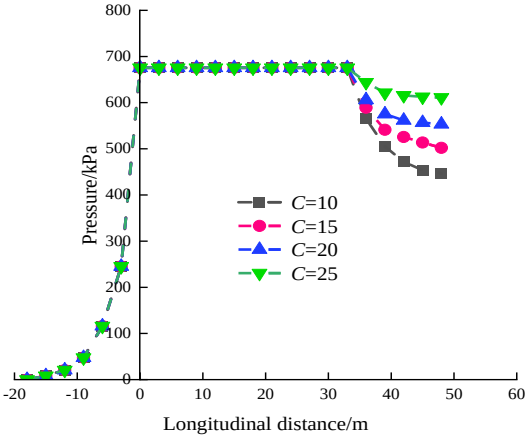

Fig. 15 Effects of C on contact loads between surrounding rock and primary support

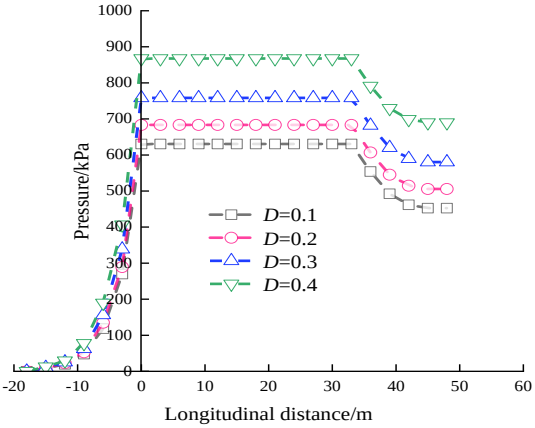

Fig. 16 Effects of D on contact loads between surrounding rock and primary support

1.633, respectively. It can be done by assuming that the other parameters remain unchanged and varying one of the parameters of λ_0, $u(\infty)$, A, C and D, the results can be obtained as shown in Fig. 12 to Fig. 16.

From Fig. 12, it is obvious to see that the contact load between the surrounding rock and the primary support varies according to the envisaged path, which indicates a trend of increasing-unchanged-decreasing-stable. The larger λ_0 is, the larger the contact load will be. For every 0.05 increase in λ_0, the contact load increases by more than 100kPa. From Fig. 13, it can be seen that the final deformation of the surrounding rock has a large effect on the contact loads between surrounding rock and primary support. The increase of u_∞ by more than 50 mm increases the contact load by not less than 300 kPa, and the increase gradually decreases. Moreover, in the deceleration stage of the surrounding rock, the larger u_∞ is, the less the contact load decreases. As for the effects of some constants on the contact loads between surrounding rock and primary support, Figs. 14-16 illustrate the effects of A, C and D on the contact loads between surrounding rock and primary support. The effects of A and C on the contact load are similar, and all of them affect the final contact loads between surrounding rock and primary support in the stage of deceleration of the surrounding rock. In addition, the larger D is, the larger the contact loads between surrounding rock and primary support will be, and the load increases by 50 kPa to 100 kPa for every 0.1 increase in D. The larger the value of D is, the larger the increase in load will appear. The effect of D on contact load is greater than A and C by sensitivity comparison of constants.

In summary, the values of λ_0 and D are as small as possible to reduce the deformation of the surrounding rock during the pre-deformation phase which can avoid large contact loads between surrounding rock and primary support. For weak surrounding rock tunnels, the values of λ_0 and D can be reduced by installing advanced support.

Figs. 17-19 show the effect of shotcrete thickness t_c, elastic modulus E_1 and spacing of steel arch arrangement S on the contact loads between surrounding rock and primary support, respectively. It is not difficult to find that the relationship between t_c and the contact loads present a nonlinear relationship, and the larger t_c is, the larger the contact load will appear. The larger the final deformation of surrounding rock, the more obvious with the increase of thickness. For weak surrounding rock tunnels, the thickness of shotcrete on site is generally greater than 20 cm.Then, the final deformation of the surrounding rock increases by 50 mm, the contact loads increase by more than 200 kPa. The relationship between E_1 and contact loads shows a linear relationship, and the trend of E_1 and contact loads are more consistent with t_c. The elastic modulus of shotcrete in the field is generally 25 GPa, then every 50 mm increase in the final deformation of the surrounding rock, the contact loads increase more than 200 kPa. S and the contact loads show an inverse proportional relationship, the larger the S, the smaller the contact load, and the larger the final deformation of the surrounding rock, the more obvious the contact load decreases.

Overall, if the deformation produced by the surrounding rock is larger at higher shotcrete thickness or elastic modulus, it indicates that the quality of the surrounding rock is poorer, and the larger the contact loads between surrounding rock and primary support are produced. On the other hand, when other conditions remain unchanged, the

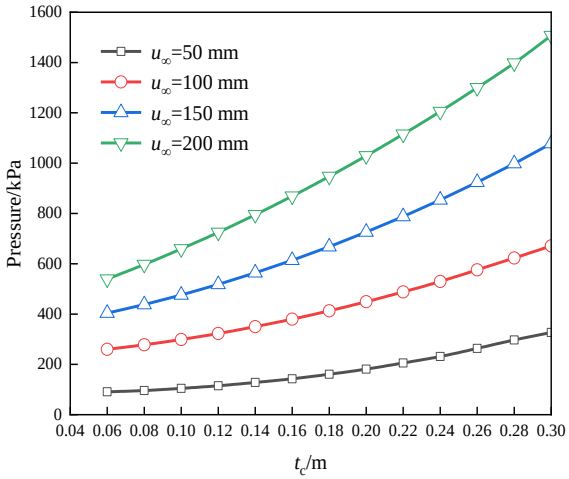

Fig. 17 Effects of t_c on contact loads between surrounding and primary support

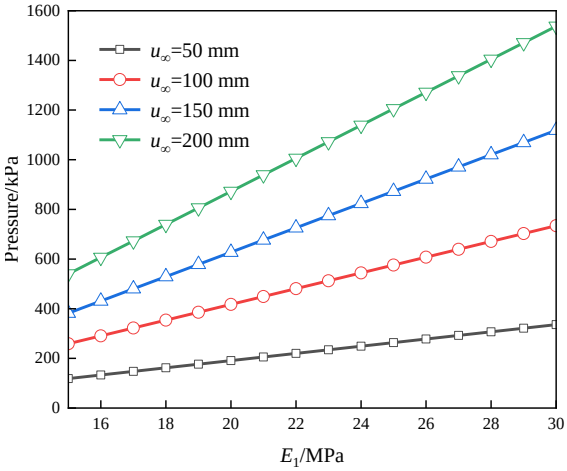

Fig. 18 Effects of E_1 on contact loads between surrounding rock and primary support

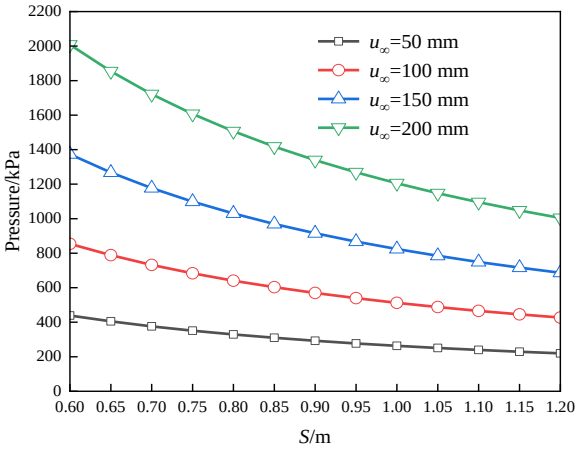

Fig. 19 Effects of S on contact loads between surrounding rock and primary support

higher the shotcrete strength or thickness, the smaller the final deformation of the surrounding rock, while the contact load does not change significantly. In addition, the larger the spacing of the steel arch, the resulting deformation of

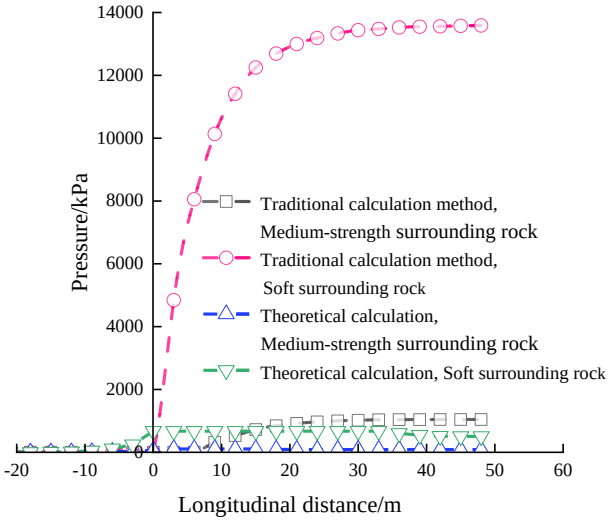

Fig. 20 Comparison of traditional calculation method with the method of this study

the surrounding rock will also show a tendency to increase. Then the effect of the steel arch's installation of the contact load is smaller. However, weakening the support parameters will inevitably result in large surrounding rock deformations that pose a threat to tunnel safety. If the safety factor of the support structure is reduced, it is not desirable for weak surrounding rock tunnels.

6. Discussion

The calculation method of contact load between surrounding rock and primary support proposed in this study is a novel solution for surrounding rock pressure. As we know, the pressure box is often installed between the surrounding rock and the primary support in the engineering site to measure the surrounding rock pressure (Luo *et al.* 2022). In the past, the calculation method of surrounding rock pressure often used Terzaghi formula, Protodyakonov's theory or the formula summarized in the specification (Tong 2020, Hu *et al.* 2022). These methods are empirical which have limited parameters that do not reflect the complete tunnel construction process. Thus, for a particular project, the prediction of these formulas is often biased. In addition, a more serious problem is that for deep-buried tunnels, the surrounding rock has a certain self-supporting capacity, and the contact load between the surrounding rock and the primary support is often smaller than that of shallow tunnels. The main reason for this is that the support structure of shallow tunnels carries the self-weight of the rock overlying the tunnel (Zhang *et al.* 2014). Its self-supporting capacity is much weaker than that of deep-buried tunnels, and there is almost no self-supporting capacity in soft strata. Therefore, the traditional empirical formulae are often not applicable to deep-buried tunnels.

The previous method of calculating the surrounding rock pressure in deep tunnels was actually an ultimate support pressure. The traditional calculation method can be compared with the method of this study considering flexible

support. The design parameters are consistent with Section IV, as shown in Fig. 20. It is not difficult to find that the difference between the traditional calculation method and the method of this study is large, and the worse the surrounding rock conditions, the more obvious this gap. Thus, the maximum value of the calculated support to provide the reaction force does not reflect the load shared by the primary support during the whole construction process. The inversion method of surrounding rock pressure given in this study is consistent with the original design intention of flexible support, which makes up for the blank of surrounding rock pressure calculation in deep-buried tunnels.

This research is based on the inversion of the dynamic deformation curves of tunnel construction to predict the contact loads between surrounding rock and primary support, which is applicable to the prediction of the contact loads between surrounding rock and primary support in medium strength and soft rock tunnels. For hard rock tunnels, the contact load and the safety threat to the support structure all are very small, so it is not within the scope of this study for the time being. Thus, the methodology of this study is more applicable to the calculation of surrounding rock pressure in deep-buried tunnels with medium-strength or weak surrounding rock.

7. Conclusions

Based on the dynamic deformation curves of tunnel constructions, this research revealed the formation mechanism of contact loads between surrounding rock and primary support from the perspective of surrounding rock kinematics. A new method of contact loads calculation between surrounding rock and primary support was inverted. The following conclusions can be achieved.

(1) The fitting curve of surrounding rock deformation for dynamic tunnel construction is proposed to overcome the previous misconception that there exists a direct relationship between the increment of surrounding rock deformation and contact loads. It is summarized that the surrounding rock in the accelerated, uniform and decelerated stages of the contact load calculation between surrounding rock and primary support present the state of increasing, unchanged and decreasing.

(2) It is believed that the real influence on the contact loads between surrounding rock and primary support lies in the acceleration and deceleration stages of the surrounding rock. The deformation of the surrounding rock in the acceleration and deceleration stages is not completely transformed into the contact load, and the deformation of the surrounding rock when it is in uniform velocity should be subtracted.

(3) The feasibility of this research method is verified by comparing and analyzing the new method of contact load calculation between surrounding rock and primary support with numerical simulation results. The contact loads between surrounding rock and primary support of medium-strength surrounding rock tunnels and soft surrounding rock tunnels are generally within 150 kPa and 1 MPa, respectively.

(4) For weak surrounding rock tunnels, advanced support can be installed to reduce the values of λ_0 and D to achieve the purpose of reducing the contact loads between surrounding rock and primary support. On the other hand, when other conditions remain unchanged, the influences of shotcrete strength, thickness or spacing of steel arch on the contact loads between surrounding rock and primary support are small, but the change of the support parameters will inevitably have an influence on the safety factor of the support structure.

Acknowledgements

This study is sponsored by the Scientific Research Project of Zhejiang Provincial Department of Education (Y202351526) and Scientific Research Project of Zhejiang Provincial Transportation Department (2021050). The financial supports are greatly appreciated.

References

Alejano, L.R., Rodriguez-Dono, A. and Veiga, M. (2012), "Plastic radii and longitudinal deformation profiles of tunnels excavated in strain-softening rock masses", *Tunn. Undergr. Sp. Tech*., **30**(1), 169-182. https://doi.org/10.1016/j.tust.2012.02.017.

Carranza-Torres, C. (2000), "Application of the convergence confinement method of tunnel design to rock masses that satisfy the Hoek-Brown failure criterion", *Tunn. Undergr. Sp. Tech*., **15**(2),187-213. https://doi.org/10.1016/S0886-7798(00)00046-8.

Carranza-Torres, C. and Fairhurst, C. (1999), "General formulation of the elasto-plastic response of openings in rock using the Hoek-Brown failure criterion", *Int. J. Rock. Mech. Min. Sci*., **36**(6), 777-809. https://doi.org/10.1016/S0148-9062(99)00047-9.

Cai, Y., Jiang, Y.J. and Djamaluddin, I. (2015), "An analytical model considering interaction behavior of grouted rock bolts for convergence–confinement method in tunneling design", *Int. J. Rock. Mech. Min. Sci*., **76**, 112-126. https://doi.org/10.1016/j.ijrmms.2015.03.006.

Chinaei, F., Ahangari, K. and Shirinabadi, R. (2021), "Hoek-Brown failure criterion for damage analysis of tunnels subjected to blast load", *Geomech. Eng.* **26**(1), 41-47. https://doi.org/10.12989/gae.2021.26.1.041.

Dehnavi, R.N. and Sadeghi, M. (2019), "Deterioration of weak rocks over time and its effect on designing tunnel support systems", *B. Eng. Geol. Environ*., **78**(2), 1045-1056. https://doi.org/10.1007/s10064-017-1154-9.

Fahimifar, A., Ghadami, H. and Ahmadvand, M. (2015). "The ground response curve of underwater tunnels, excavated in a strain-softening rock mass". *Geomech. Eng.* **8**(3), 323-359. https://doi.org/10.12989/gae.2015.8.3.323.

Fan, S.Y., Song, Z.P., Xu, T., Wang, K.M. and Zhang, Y.W. (2021), "Tunnel deformation and stress response under the bilateral foundation pit construction: a case study", *Arch. Civ. Mech. Eng*., **21**(3), 109. https://doi.org/10.1007/s43452-021-00259-7.

Feng, Q., Jiang, B.S. and Zhang, Q. (2014), "Analytical elasto-plastic solution for stress and deformation of surrounding rock in cold region tunnels", *Cold. Reg. Sci. Technol.*, **108**, 59-68. https://doi.org/10.1016/j.coldregions.2014.08.001.

Guo, Z.Z., Qiu, D.H., Yu, Y.H., Xue, Y.G., Liu, Q.S., Zhang, W.M. and Li, Z.Q. (2023), "Analysis and prediction of nonuniform deformation in composite strata during tunnel excavation",

Comput. Geotech., **157**, 105338. https://doi.org/10.1016/j.compgeo.2023.105338.

Hoek, E. (2001), "The role of experts in tunneling experience from Greece and the world", Keynote ecture, Iaonnina, Egnatia Odos Tunnelling Conference.

Hu, J., He, M.C., Li, H.R., Tao, Z.G., Liu, D.Q., Cheng, T. and Peng, D. (2023), "Rockburst hazard control using the excavation compensation method (ECM): a case study in the Qinling water conveyance tunnel", *Eng*., 1-17. https://doi.org/10.1016/j.eng.2023.11.013.

Hu, Z., Zhang, J.W., Yang, Y.T., Wang, Z.C., Xie, Y.L., Qiu, J.L., He, S.Y. and Wang, X.L. (2022), "Study on the surrounding rock pressure characteristics of loess tunnel based on statistical analysis in China", *Appl. Sci*., **12**(13), 6329. https://doi.org/10.3390/app12136329.

Liu, J.H., Liu, X.M., Zhang, Y.J. and Xiao, T. (2015), "Numerical analysis and field monitoring tests on shallow tunnels under weak surrounding rock", *J. Cent. South. Univ.* **22**(10), 4056-4063. https://doi.org/10.1007/s11771-015-2950-7.

Liu, W.W., Feng, Q., Fu, S.G. and Wang, C.X. (2018), "Elasto-plastic solution for cold-regional tunnels considering the compound effect of non-uniform frost heave, supporting strength and supporting time", *Tunn. Undergr. Sp. Tech*., **82**, 293-302. https://doi.org/ 10.1016/j.tust.2018.08.054.

Luo, J.W., Zhang, D.L., Sun, Z.Y., Fang, Q., Liu, D.P., Xu, T. and Li, R. (2022), "Numerical modelling and field monitoring study on large-span tunnelling using pretensioned bolt-cable combined support system", *Tunn. Undergr. Sp. Technol*., **132**, 104911. https://doi.org/10.1016/j.tust.2022.104911.

Miranda, T., Dias, D., Pinheiro, M. (2015), "Methodology for real-time adaptation of tunnels support using the observational method", *Geomech. Eng*., **8**(2), 153-171. https://doi.org/10.12989/gae.2015.8.2.153.

Moon, J.S., An, J.W., Kim, H.K., Lee, J.G. and Lattner, T. (2022), "Evaluation criteria for freezing and thawing of tunnel concrete lining according to theoretical and experimental analysis", *Geomech. Eng.*, **29**(3), 349-357. https://doi.org/10.12989/gae.2022.29.3.349.

Oreste, P.P. (2003a), "A procedure for determining the reaction curve of shotcrete lining considering transient conditions", *Rock. Mech. Rock. Eng*., **36**(3), 209-236. https://doi.org/10.1007/s00603-002-0043-z.

Oreste, P.P. (2003b), "Analysis of structural interaction in tunnels using the convergence–confinement approach", *Tunn. Undergr. Sp. Tech*., **18**, 347-363. https://doi.org/10.1016/S0886-7798(03)00004-X.

Park, K.H. and Kim, Y.J. (2006), "Analytical solution for a circular opening in an elastic-brittle-plastic rock", *Int. J. Rock. Mech. Min. Sci*., **43**(4), 611-622. https://doi.org/10.1016/j.ijrmms.2005.11.004.

Panet, M. (1995), "Le Calcul des tunnels par la méthode de convergence-confinement", Paris: Press de l'école Nationale des Ponts et Chaussées.

Prassetyo, S.H. and Gutierrez, M. (2018), "Effect of transient coupled hydro-mechanical response on the longitudinal displacement profile of deep tunnels in saturated ground", *Tunn. Undergr. Sp. Tech*., **75**, 11-20. https://doi.org/10.1016/j.tust.2018.02.003.

Serrano, A., Olalla, C. and Reig, I. (2011), "Convergence of circular tunnels in elastoplastic rock masses with non-linear failure criteria and non-associated flow laws", *Int. J. Rock. Mech. Min. Sci*., **48**(6), 878-887. https://doi.org/10.1016/j.ijrmms.2011.06.008.

Rabcewicz, L.V. (1964), "The new Austrian tunnelling method", *Water. Power*, **17**(1), 511-515.

Ranjbarnia, M., Rahimpour, N. and Oreste, P. (2020), "A new analytical-numerical solution to analyze a circular tunnel using 3D Hoek-Brown failure criterion", *Geomech. Eng.*, **22**(1), 11-23. https://doi.org/10.12989/gae.2020.22.1.011.

Shen, Q., Zheng, J.J., Cui, L., Pan, Y. and Cui, B. (2019), "A procedure for interaction between rock mass and liner for deep circular tunnel based on new solution of longitudinal displacement profile", *Eur. J. Environ. Civ. Eng.*, **26**(1), 280-298. https://doi.org/10.1080/19648189.2019.1657960.

Sun, M.S., Ma, T., Shen, Z.J., Wu, X. and Wang, M.S. (2018), "Study of lining sharing surrounding rock pressure in composite lining", *Rock. Soil. Mech.*, **39**(S1), 437-445.

Tian, X.X., Song, Z.P., Wang, H.Z., Zhang, Y.W. and Wang, J.B. (2022), "Evolution characteristics of the surrounding rock pressure and construction techniques: A case study from Taoshuping tunnel", *Tunn. Undergr. Sp. Tech.*, **125**, 104522. https://doi.org/10.1016/j.tust.2022.104522.

Tong, J.S. (2020), "General formulas for calculating surrounding rock pressure of tunnels and underground spaces", *KSCE. J. Civ. Eng*., **24**(4), 1348-1356. https://doi.org/10.1007/s12205-020-0943-z.

Vlachopoulos, N. and Diederichs, M.S. (2009), "Improved longitudinal displacement profiles for convergence confinement analysis of deep tunnels", *Rock. Mech. Rock. Eng*., **42**(2), 131-146. https://doi.org/10.1007/s00603-009-0176-4.

Zhang, B.Q., Chen, F.Q. and Wang, Q.Y. (2019), "Elastoplastic solutions for surrounding rock masses of deep-buried circular tunnels with non-darcian flow", *Int. J. Geomech.*, **19**(7), 1-12. https://doi.org/10.1061/(ASCE)GM.1943-5622.0001442.

Zhang, D.L. and Chen, L.P. (2016), "Compound structural characteristics and load effect of tunnel surrounding rock", *Chi. J. Rock. Mech. Eng.*, **35**(3), 456-469. (in Chinese)

Zhang, S.C., Mu, C.M., Feng, X.H., Ma, K., Guo, X. and Zhang, X.S. (2024), "Intelligent dynamic warning method of rockburst risk and level based on recurrent neural network", *Rock. Mech. Rock. Eng.*, Early Access. https://doi.org/ 10.1007/s00603-023-03715-3.

Zhang, Z.Q., Li, H.Y., Liu, H.Y., Li, G.J. and Shi, X.Q. (2014), "Load transferring mechanism of pipe umbrella support in shallow-buried tunnels", *Tunn. Undergr. Space Tech*., **43**, 213-221. https://doi.org/10.1016/j.tust.2014.05.018.

Zhang, Y.J., Su, K., Qian, Z.D. and Wu, H.G. (2019), "Improved longitudinal displacement profile and initial support for tunnel excavation", *KSCE. J. Civ. Eng*., **23**(6), 2746-2755. https://doi.org/10.1007/s12205-019-0411-9.

Zhou, J. and Yang, X.A. (2021a), "An analysis of the support loads on composite lining of deep-buried tunnels based on the Hoek-Brown strength criterion", *Tunn. Undergr. Sp. Tech*., **118**, 104174. https://doi.org/10.1016/j.tust.2021.104174.

Zhou, J., Yang, X.A., Ma, M.J. and Li, L.H. (2021b), "The support load analysis of deep-buried composite lining tunnel in rheological rock mass", *Comput. Geotech.*, **130**, 103934. https://doi.org/10.1016/j.compgeo.2020.103934.

Zhou, J., Yang, X.A. and Chu, Z. (2023a), "Load laws of composite lining in mountain tunnel model tests and numerical simulation validation", *J. Mountain. Sci*., **20**(7), 2041-2057. https://doi.org/10.1007/s11629-023-8043-4.

Zhou, J., Yang, X.A. and Ding, Z. (2023b), "A secondary development based on the Hoek-Brown criterion for rapid numerical simulation prediction of mountainous tunnels in China", *Geomech. Eng.*, **34**(1), 69-86. https://doi.org/10.12989/gae.2023.34.1.069.

IC